JOURNAL of the MEXICAN CHEMICAL SOCIETY

https://www.jmcs.org.mx/

Article

Open Access

J. Mex. Chem. Soc. **2026**, *70(1):e2527*

Received August 4th, 2025
Accepted February 12th, 2026

http://dx.doi.org/10.29356/jmcs.v70i1.2527
e-location ID: 2527

Keywords:
Alkoxyl radicals, Organic electrosynthesis, *N*-alkoxyphthalimides (NAPIs), *C-H* allylation, δ-functionalization

Palabras clave:
Radicales alcoxilo, Electrosíntesis orgánica, *N*-alcoxiftalimidas, Alilación *C-H*, Funcionalización δ

***Corresponding author:**
Julio Romero-Ibañez
email: julio.romero@iquimica.unam.mx
Bernardo A. Frontana-Uribe
email: bafrontu@unam.mx

ISSN-e 2594-0317

Electrogeneration of *O*-centered Radicals from *N*-alkoxyphthalimides and their use in δ-C-H functionalization. Comparison with the Photocatalytic Redox reaction

Edgar A. Colindres-Diaz[1], Diego Francisco Chicas-Baños[2,3], Julio Romero-Ibañez[1,2]*, Bernardo A. Frontana-Uribe[1,2,]*

[1]Centro Conjunto de Investigación en Química Sustentable UAEMex-UNAM, Km. 14.5 Carretera Toluca-Atlacomulco, Toluca, C.P. 50200, Estado de México, México.
[2]Instituto de Química, Universidad Nacional Autónoma de México, Circuito exterior, Coyoacán, Ciudad de México.
[3]Facultad de Ciencias Naturales y Matemática, Escuela de Química, Universidad de El Salvador (UES), San Salvador, El Salvador.

Abstract. The alkoxyl radicals have been proved to be useful synthetic intermediates in the δ-functionalization of *C-H* bonds, and their generation has progressed from the traditional harsh and toxic environments to benign reaction conditions provided by photoredox catalysis (PRC) and organic electrosynthesis (OES). This work describes the findings related to the reductive electrogeneration of oxygen-centered radicals from *N*-alkoxyphthalimides (NAPIs) and their use in remote *C-H* allylation. In this approach, the use of pulsed alternating polarity electrolysis, Hantzsch ester in the presence of *δ*-terpinene as a proton donor and hydrogen donor, respectively, in combination of an allyl sulfone led us to achieve the consecutive cathodic reduction, *N-O* cleavage, 1,5-hydrogen atom transfer, and radical allylation. Finally, the synthesized NAPIs were subjected to standard photocatalytic redox conditions, yielding comparable results.

J. Mex. Chem. Soc. **2026**, *70(1):e2527*
Regular Issue

ISSN-e 2594-0317

Resumen. Los radicales alcoxilo han demostrado ser intermediarios sintéticos útiles en la funcionalización δ de enlaces *C–H*, y su generación ha evolucionado desde ambientes tradicionales severos y tóxicos hacia condiciones de reacción benignas proporcionadas por la catálisis fotoredox y la electroquímica orgánica. Este trabajo describe los hallazgos relacionados con la electrogeneración reductiva de radicales centrados en oxígeno a partir de *N*-alcoxiftalimidas y su uso en la alilación remota de enlaces *C–H*. En este estudio, el uso de electrólisis con polaridad alternante pulsada, éster de Hantzsch en presencia de γ-terpineno como donadores de protón e hidrógeno, respectivamente, en combinación con una alilsulfona, nos permitió lograr la reducción catódica, ruptura del enlace *N–O*, transferencia de átomo de hidrógeno 1,5 y alilación radicalaria. Finalmente, las *N*-alcoxiftalimidas sintetizadas se hicieron reaccionar en condiciones estándar de catálisis foto-redox, obteniéndose resultados comparables.

Introduction

Alkoxyl radicals are useful intermediates in organic synthesis, [1,2] depending on their structure and environment, [3,4] they can react following different mechanisms: addition to an activated double bond, [5,6] β-scission, [7,8] or hydrogen atom transfer (HAT) process [9,10]. The latter has attracted the attention of the synthetic community because of the possibility of functionalizing inactivated *C-H* bonds. Though the relatively high bond dissociation energy (BDE) of alkyl *C-H* bonds (95-101 kcal/mol) [11], thermodynamically, alkoxyl radicals could promote the generation of carbon-centered radicals *via* an intra- or intermolecular HAT course (Scheme 1**(a)**).[12]

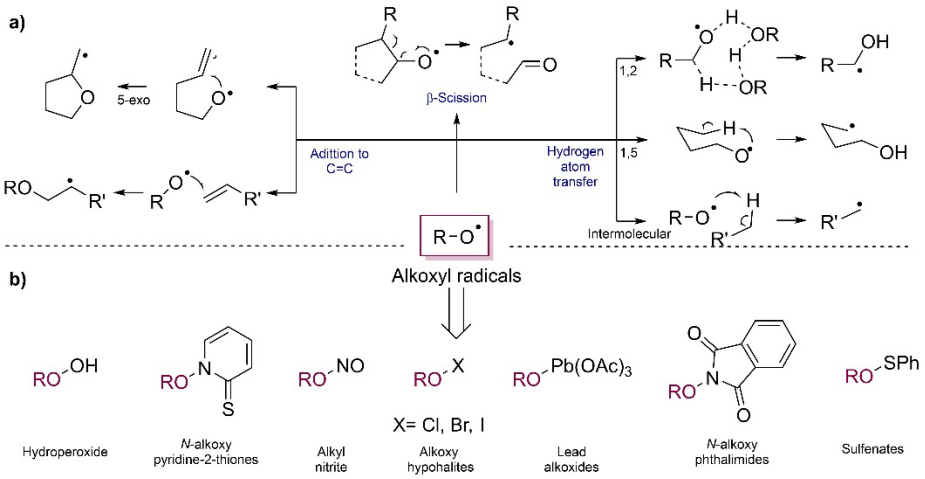

Scheme 1. (a) Reaction modes of alkoxyl radicals. **(b)** Classic precursors of alkoxyl radicals.

The homolytic *O-X* bond cleavage is the classical method for producing alkoxyl radicals; nevertheless, the actual search for sustainable methodologies in organic synthesis has evaded their employment due to the harsh, toxic, and dangerous conditions required to prepare the low-stable precursors and promote the *O-X* cleavage.[12,13] Conversely, the representative BDE of *O-H* (103-106 kcal/mol) [11] and the strong oxidants required for the direct generation of *O*-centered radicals have restricted the limits of the strategy as depicted in Scheme 1**(a)**. Over the extensive precursors employed for the generation of alkoxyl radicals, *N*-alkoxyphthalimides (NAPIs) are commonly employed due to their stability and ease of preparation (Scheme 1**(b)**).[14,15] In pursuit of more sustainable synthetic methods, recent efforts have focused on replacing traditional approaches for generating alkoxyl radicals from NAPIs, which have historically relied on organotin hydrides.[16,17] Due to their well-known toxicity and harsh generation conditions, stannyl radicals have been

http://dx.doi.org/10.29356/jmcs.v70i1.2527

J. Mex. Chem. Soc. **2026**, *70(1):e2527*
Regular Issue

ISSN-e 2594-0317

replaced by organosilyl reagents[18], and catalytic photosensitizers activated by visible light.[12] Since then, photocatalytic redox chemistry has dramatically expanded the use of alkoxyl radicals in structural modification and the synthesis of valuable natural and bioactive products.[1] Although electrochemical methods align well with several principles of green chemistry,[19,20] the use of electricity to generate alkoxyl radicals from NAPIs remains underexplored, with only a few initial reports emerging that begin to clarify their generation and reactivity.[21-24]

Fostering on the primary studies of Terent'ev group,[21] it was demonstrated the efficiency in accessing carbonyl compounds from *N*-benzyloxyphthalimides (NBOPIs) through a cathodic reaction of substrates bearing this aromatic heterocyclic redox reactive motif (Scheme 2**(a)**).[22] Later, the conversion of NAPIs to *O*-centered radicals was modulated under electroreductive conditions by employing the Hantzsch ester (**HE**) and rapid alternating polarity (RAP) electrolysis (Scheme 2**(b)**).[23] This methodology involves a variety of paired electrosynthesis, where both electrodes alternate their polarity over a specified time period.[25] In this latter research, as for the photocatalytic generation of alkoxyl radical from NAPIs reported by Chen *et al*,[26] the oxidized **HE** (cation radical) played a critical role in promoting the *N-O* cleavage of the radical anion **A**, meanwhile, the RAP technique let the nearby generation of the entities $\mathbf{HE}^{\bullet+}$ and **A** avoiding the formation of carbonyl substrates. To prove the formation of the alkoxyl radical, the NAPI **3a** bearing a δ-C-H bond liable to forming a stabilized carbon radical via a 1,5-HAT process, led to the obtention of the allylated product **4a** (Scheme 2**(c)**).[23]

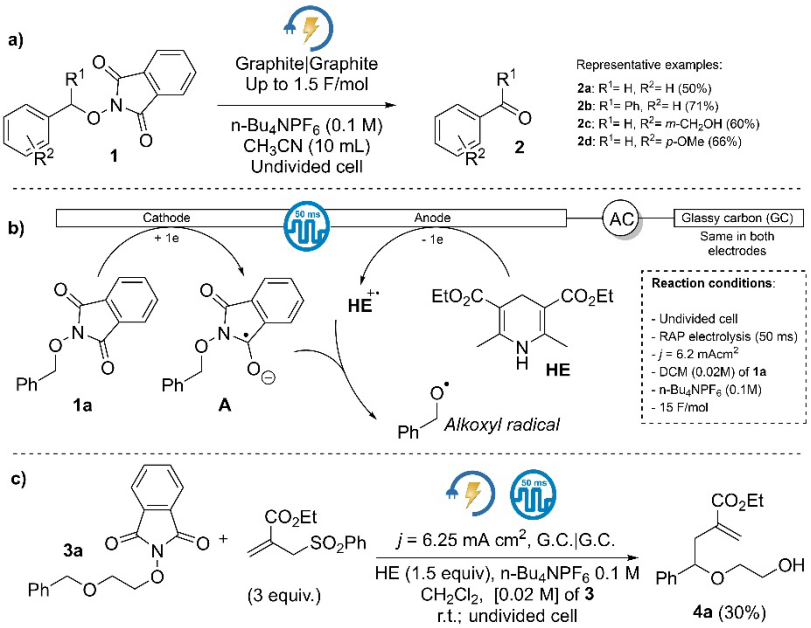

Scheme 2. (a) Electroreduction of NBOPIs **1** to generate carbonyl compounds. **(b)** Electroreduction of NAPI **1a** to generate alkoxyl radicals. **(c)** Remote C-H allylation of the chain using NAPI **3a**.

With the establishment of OES as a sustainable alternative to toxic and dangerous traditional reaction conditions, the translation of photocatalytic redox conditions for generating alkoxyl radicals into electrochemical platforms aligns with the scientific community's ongoing efforts to replace expensive metal-based catalysts, such as iridium, due to their scarcity and demand.[27] In this context, the development of modern electrochemical equipment, such as the ElectraSyn reactor, now enables the straightforward implementation of advanced electrolysis modes, including rapid and pulsed alternating polarity programs, thereby opening new opportunities to explore unconventional reactivity in OES. Accordingly, the findings reported regarding the electrogeneration of alkoxyl radicals from NAPIs and their subsequent remote *C-H* allylation are particularly appropriate. Therefore, our attention was focused on the stereoelectronic nature of the benzylic structure, where a transient nucleophilic carbon radical is formed, as this site may favor a one-electron

J. Mex. Chem. Soc. **2026**, *70(1):e2527*
Regular Issue

ISSN-e 2594-0317

oxidation pathway leading to byproducts. In this regard, understanding this classical reaction pathway can open the door to more complex scenarios or the synthesis of compounds of biological or pharmaceutical relevance.

Experimental

Commercially available reagents were used without further purification. Unless otherwise noted, reactions were carried out under an inert argon atmosphere with dry solvents under anhydrous conditions. Solvents were used as technical grade, and freshly distilled prior to use. Column chromatography (CC) was performed using silica gel (70-230 mesh) with solvents indicated in the text. Melting points were not corrected and carried out on a Fisher-Scientific 12-144 melting point apparatus. NMR spectra were recorded on Bruker (300 MHz, Avance) and Bruker (500 MHz, Ascend) using TMS as an internal reference for ^{1}H (0.0 ppm) and $CDCl_3$ for ^{1}H (7.26 ppm), and ^{13}C (77.16 ppm); chemical shifts (δ) are stated in parts per million (ppm) and Hz for the coupling constants (*J*). The following abbreviations (or combinations thereof) were used to explain the multiplicities: s = singlet, d = doublet, t = triplet, q = quartet, m = multiplet, br = broadened. High resolution mass spectra-Electrospray ionization mode (HRMS-ESI). Voltammetric studies were carried out using a PGSTAT204 Potentiostat and a conventional glass cell of 10 mL. Reference electrode: Ag/Ag^{+} (filled with $AgNO_3$ 0.01 M in CH_3CN). Working electrode: glassy carbon disk (diameter: 3mm). Counter electrode: platinum wire (99.95 % purity). Preparative electrolysis was carried out using an ElectraSyn 2.0 in a 10 mL glass cell. Electrodes: Platinum (Pt), and Glassy carbon (GC). Photoredox reactions were carried out using an EvoluChem PhotoRedOx Box reactor and EvoluChem LED 450PF non-dimmable 110V-220V (PF series light 18W; 328 mW/cm^2).

Synthesis of *N*-alkoxyphthalimides 3a-3e

The general strategy for preparing the *N*-alkoxyphthalimides **3a-3d** was as follows: benzylation of ethylene glycol framework followed by the insertion of *N*-hydroxyphthalimide moiety *via* a Mitsunobu approach (Scheme 3**(a)**). Meanwhile, the NAPI **3e** was prepared from indole-3-carboxaldehyde in a five-step protocol: first, the N-H protection-carbonyl reduction sequence gave the 3-hydroxymethyl-indole **5e** in good yield; next, the hydroxyl alkylation-ester reduction sequence afforded the alcohol **6e**; finally, the insertion of the redox active *N*-hydroxyphthalimide moiety under Mitsunobu conditions furnished the NAPI **3e** (Scheme 3**(b)**).

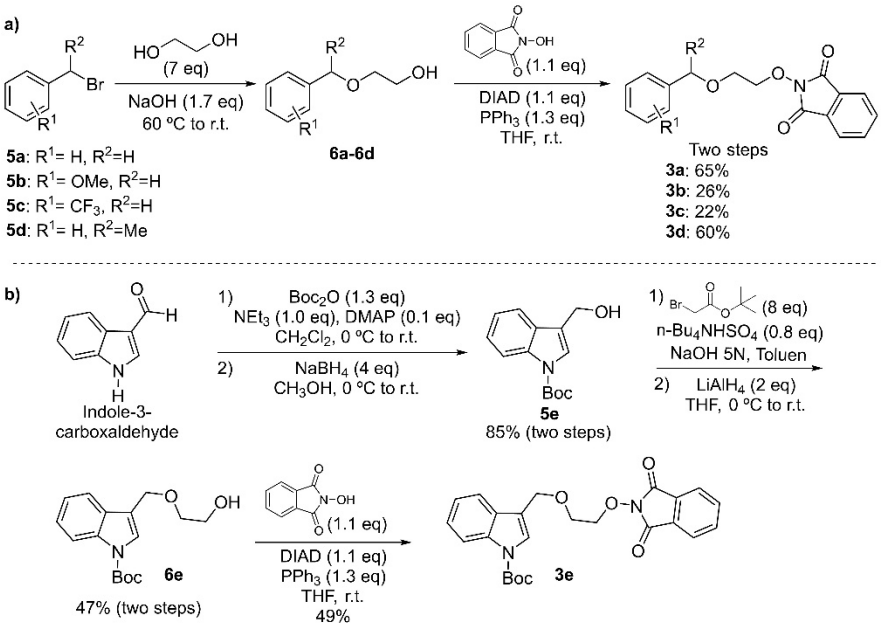

Scheme 3. Synthesis of *N*-alkoxyphthalimides **3a**-**3e**.

J. Mex. Chem. Soc. **2026**, *70(1):e2527*
Regular Issue

ISSN-e 2594-0317

Physical and spectroscopic data for *N*-alkoxyphthalimides and intermediates

2-(2-(Benzyloxy)ethoxy)isoindoline-1,3-dione (3a): White solid, m.p.: 50-53 °C. ^{1}H NMR (300 MHz, $CDCl_3$) δ: 3.86-3.88 (m, 2H), 4.41-4.42 (m, 2H), 4.55 (s, 2H), 7.22-7.26 (m, 5H), 7.72 (dd, *J* = 3.3, 1.8 Hz, 2H), 7.81 (dd, *J* = 3.3, 1.8 Hz, 2H); ^{13}C NMR (75 MHz, $CDCl_3$) δ: 68.6, 73.6, 77.2, 123.6(2C), 127.7, 127.9(2C), 128.4(2C), 129.1(2C), 134.5(2C), 137.9, 163.6(2C). HRMS (ESI-TOF) m/z: $[M+H]^+$ calcd for $C_{17}H_{16}NO_4$, 298.10793; found, 298.10650.

2-(2-((4-Methoxybenzyl)oxy)ethoxy)isoindoline-1,3-dione (3b): White solid; m.p. 84-87 ºC. NMR corresponded to data reported by Chen *et al*.[26] ^{1}H NMR (300 MHz, $CDCl_3$) δ: 3.77 (s, 3H), 3.81-3.84 (m, 2H), 4.38-4.40 (m, 2H), 4.47 (s, 2H), 6.79 (d, *J* = 8.4 Hz, 2H), 7.19 (d, *J* = 8.7 Hz, 2H), 7.70-7.74 (m, 2H), 7.77-7.81 (m, 2H); ^{13}C NMR (75 MHz, $CDCl_3$) δ: 55.4, 68.3, 73.2, 77.2, 113.8(2C), 123.6(2C), 129.1(2C), 129.5(2C), 130.0, 134.5(2C), 159.3, 163.6(2C).

2-(2-((4-(Trifluoromethyl)benzyl)oxy)ethoxy)isoindoline-1,3-dione (3c): White solid; m.p. 74-77 ºC. ^{1}H NMR (300 MHz, $CDCl_3$) δ: 3.89-3.92 (m, 2H), 4.42-4.45 (m, 2H), 4.60 (s, 2H), 7.36 (d, *J* = 8.1 Hz, 2H), 7.49 (d, *J* = 8.1 Hz, 2H), 7.69-7.73 (m, 2H), 7.75-7.79 (m, 2H); ^{13}C NMR (75 MHz, $CDCl_3$) δ: 69.2, 72.7, 77.1, 123.6(2C), 124.3 (q, J_{C-F} = 270 Hz), 125.3 (q, J_{C-F} = 3.75 Hz, 2C), 127.7(2C), 129.0(2C), 129.8 (q, J_{C-F} = 32.3 Hz), 134.5(2C), 142.0, 163.6(2C). HRMS (ESI-TOF) m/z: $[M+H]^+$ calcd for $C_{18}H_{15}F_3NO_4$, 366.09532; found, 366.09503.

2-(2-(1-Phenylethoxy)ethoxy)isoindoline-1,3-dione (3d): White solid; m.p. 63-67 ºC. ^{1}H NMR (300 MHz, $CDCl_3$) δ: 1.33 (d, *J* = 6.3 Hz, 3H), 3.64 (ddd, *J* = 11.7, 5.1, 2.7 Hz, 1H), 3.74 (ddd, *J* = 12.0, 6.9, 3.0 Hz, 1H), 4.32 (ddd, *J* = 11.7, 5.1, 3.0 Hz, 1H), 4.39 (ddd, *J* = 12.0, 6.9, 3.0 Hz, 1H), 4.46 (q, *J* = 6.6 Hz, 1H), 7.23-7.33 (m, 5H), 7.74-7.78 (m, 2H), 7.82-7.88 (m, 2H); ^{13}C NMR (75 MHz, $CDCl_3$) δ: 23.8, 67.1, 77.16, 78.7, 123.6(2C), 126.4(2C), 127.6, 128.6(2C), 129.2(2C), 134.5(2C), 143.3, 163.6(2C). HRMS (ESI-TOF) m/z: $[M+H]^+$ calcd for $C_{18}H_{18}NO_4$, 312.12358; found, 312.12226.

***Tert*-butyl 3-(hydroxymethyl)-1*H*-indole-1-carboxylate (5e):** White solid, m.p.: 68-72 ºC. NMR corresponded to data reported by Vanderwal *et al*.[28] ^{1}H NMR (300 MHz, $CDCl_3$) δ: 1.60 (br, 1OH), 1.67 (s, 9H), 4.84 (d, *J* = 5.4 Hz, 2H), 7.26 (td, *J* = 7.2, 1.2 Hz, 1H), 7.34 (td, *J* = 7.2, 1.2 Hz, 1H), 7.58 (s, 1H), 7.65 (d, *J* = 7.8 Hz, 1H), 8.14 (d, *J* = 8.7 Hz, 1H); ^{13}C NMR (75 MHz, $CDCl_3$) δ: 28.3, 57.4, 83.9, 115.5, 119.4, 120.6, 122.9, 123.9, 124.8, 129.3, 135.9, 149.8.

***Tert*-butyl 3-((2-hydroxyethoxy)methyl)-1*H*-indole-1-carboxylate (6e):** Colorless oil. NMR corresponded to data reported by Chen *et al*.[26] ^{1}H NMR (300 MHz, $CDCl_3$) δ: 1.67 (s, 9H), 3.61-3.64 (m, 2H), 3.74 (br s, 2H), 4.72 (s, 2H), 7.26 (td, *J* = 7.2, 1.5 Hz, 1H), 7.34 (td, *J* = 7.2, 1.2 Hz, 1H), 7.58 (s, 1H), 7.64 (d, *J* = 7.5 Hz, 1H), 8.14 (d, *J* = 8.4 Hz, 1H); ^{13}C NMR (75 MHz, $CDCl_3$) δ: 28.3(3C), 62.1, 65.1, 71.2, 84.0, 115.5, 117.5, 119.6, 122.9, 124.8, 124.9 129.8, 135.9, 149.8.

***Tert*-butyl 3-((2-((1,3-dioxoisoindolin-2-yl)oxy)ethoxy)methyl)-1*H*-indole-1-carboxylate (3e)**: White solid; m.p. 117-120 ºC. NMR corresponded to data reported by Chen *et al*.[26] ^{1}H NMR (300 MHz, $CDCl_3$) δ: 1.67 (s, 9H), 3.87-3.90 (m, 2H), 4.38-4.41 (m, 2H), 4.70 (s, 2H), 7.21 (td, *J* = 7.5, 1.5 Hz, 1H), 7.29 (td, *J* = 7.2, 1.2 Hz, 1H), 7.51 (s, 1H), 7.62 (d, *J* = 7.8 Hz, 1H), 7.65-7.68 (m, 2H), 7.73-7.76 (m, 2H), 8.08 (d, *J* = 8.7 Hz, 1H); ^{13}C NMR (75 MHz, $CDCl_3$) δ: 28.3(3C), 65.2, 68.3, 77.2, 83.8, 115.3, 117.4, 119.8, 122.8, 123.5(2C), 124.6, 124.8, 129.0(2C), 129.7, 134.4(2C), 135.7, 149.7, 163.6(2C).

C-H allylation of *N*-alkoxyphthalimides 3a-3e

General electrochemical procedure

In an ElectraSyn 10 mL glass-vial with a stir-bar was put n-Bu_4NPF_6 (95 %; 0.6 mmol, 0.1 M), Hantzsch ester (0.3 mmol), ethyl 2-((phenylsulfonyl)-methyl)acrylate (0.9 mmol), and *N*-alkoxyphthalimide (0.3 mmol). The IKA cell cap equipped with two standard platinum electrodes was laid. Then, 6 mL of dry dichloromethane was added (0.5 mL extra to compensate for evaporation), and the solution was stirred and degassed with nitrogen for 5 minutes. The reaction was carried out with the following experiment programming: Pulse Alternating Polarity; Upper +7.0 mA; j = 6.3 mA cm^{-2}, Upper pol time = 20s; Lower -7.0 mA; j = 6.3 mA cm^{-2}, Lower pol time = 10s, 12 F/mol, and 1000 rpm. Upon completion, the solvent was removed under reduced pressure. Then, the electrolyte was crystallized with Et_2O, and the solids were filtered and washed with Et_2O (3 × 10 mL). The ethereal phase was evaporated, and the residue was purified by column chromatography.

http://dx.doi.org/10.29356/jmcs.v70i1.2527

J. Mex. Chem. Soc. **2026**, *70(1):e2527*
Regular Issue

ISSN-e 2594-0317

General photocatalytic procedure

In a 4 mL glass-vial with a stir-bar was put $[Ir(dtbbpy)(ppy)_2]PF_6$ (1 mol%; 0.003 mmol), Hantzsch ester (0.45 mmol), ethyl 2-((phenylsulfonyl)methyl)acrylate (0.9 mmol), and *N*-alkoxyphthalimide (0.3 mmol). The vial was stopped with a septum and placed under an inert atmosphere. Then, 3 mL of dry dichloromethane was added (0.5 mL extra to compensate for evaporation), and the solution was stirred and degassed with nitrogen for 5 minutes. Then, the vial was set in the photoreactor, stirred, and irradiated with a 450nm blue-LED lamp for 3 h at 0 ºC. Afterwards, the solvent was removed under reduced pressure, and the residue was purified by column chromatography.

Physical and spectroscopic data for products

Ethyl 4-(2-hydroxyethoxy)-2-methylene-4-phenylbutanoate (**4a**-Scheme 4): Colorless oil. ^{1}H NMR (300 MHz, $CDCl_3$) δ: 1.33 (t, *J* = 7.2 Hz, 3H), 2.11 (br s, 1H), 2.68 (ddd, *J* = 14.1, 5.1, 1.2 Hz, 1H), 2.81 (ddd, *J* = 14.1, 8.4, 1.2 Hz, 1H), 3.35-3.41 (m, 1H), 3.49 (dt, *J* = 10.2, 4.2 Hz, 1H), 3.68 (br m, 2H), 4.23 (q, *J* = 7.2 Hz, 2H), 4.51 (dd, *J* = 8.4, 5.1 Hz, 1H), 5.54 (q, *J* = 1.2 Hz, 1H), 6.18 (d, *J* = 1.5 Hz, 1H), 7.27-7.39 (m, 5H); ^{13}C NMR (75 MHz, $CDCl_3$) δ: 14.3, 41.2, 60.9, 62.1, 70.2, 81.3, 126.7(2C), 127.2, 127.9, 128.6(2C), 137.6, 141.7, 167.5. HRMS (ESI-TOF) m/z: $[M+H]^+$ calcd for $C_{15}H_{21}O_4$, 265.14398; found, 265.14364.

Ethyl 4-(2-hydroxyethoxy)-4-(4-methoxyphenyl)-2-methylenebutanoate (**4b**-Scheme 4): Light-yellow oil. NMR corresponded to data reported by Chen *et al*.[26] ^{1}H NMR (300 MHz, $CDCl_3$) δ: 1.31 (t, *J* = 7.2 Hz, 3H), 2.63 (ddd, *J* = 14.1, 5.4, 1.2 Hz, 1H), 2.80 (ddd, *J* = 14.0, 8.1, 1.2 Hz, 1H), 3.34 (dt, *J* = 10.3, 4.8 Hz, 1H), 3.44 (dt, *J* = 10.4, 3.9 Hz, 1H), 3.65 (t, *J* = 4.6 Hz, 2H), 3.80 (s, 3H), 4.20 (q, *J* = 7.2 Hz, 2H), 4.44 (dd, *J* = 8.3, 5.4 Hz, 1H), 5.50 (s, 1H), 6.14 (d, *J* = 1.5 Hz, 1H), 6.85-6.90 (m, 2H), 7.19-7.29 (m, 2H); ^{13}C NMR (75 MHz, $CDCl_3$) δ: 14.3, 41.1, 55.4, 60.9, 62.1, 70.0, 80.9, 114.0(2C), 127.1, 127.9(2C), 133.7, 137.7, 159.3, 167.5.

Ethyl 4-(2-hydroxyethoxy)-2-methylene-4-(4-(trifluoromethyl)phenyl)butanoate (**4c**-Scheme 4): Light-yellow oil. ^{1}H NMR (300 MHz, $CDCl_3$) δ: 1.31 (t, *J* = 7.2 Hz, 3H), 2.02 (br, 1OH), 2.67 (ddd, *J* = 14.0, 5.2, 1.2 Hz, 1H), 2.77 (ddd, *J* = 14.0, 8.1, 1.0 Hz, 1H), 3.38 (dt, *J* = 9.9, 4.3 Hz, 1H), 3.47 (dt, *J* = 9.9, 4.2 Hz, 1H), 3.68-3.72 (m, 2H), 4.20 (q, *J* = 7.2 Hz, 2H), 4.58 (dd, *J* = 8.1, 5.4 Hz, 1H), 5.53 (s, 1H), 6.17 (d, *J* = 1.6 Hz, 1H), 7.42 (d, *J* = 8.4 Hz, 2H), 7.61 (d, *J* = 8.1 Hz, 2H); ^{13}C NMR (75 MHz, $CDCl_3$) δ: 14.4, 41.2, 61.1, 62.0, 70.6, 80.8, 124.2 (q, $J_{C\text{-}F}$ = 270 Hz), 125.6 (q, $J_{C\text{-}F}$ = 3.75 Hz, 2C), 127.0(2C), 127.7, 130.2 (q, $J_{C\text{-}F}$ = 32.3 Hz), 137.0, 145.9, 167.3. HRMS (ESI-TOF) m/z: $[M+H]^+$ calcd for $C_{16}H_{20}F_3O_4$, 333.13137; found, 333.13175.

Ethyl 4-(2-hydroxyethoxy)-2-methylene-4-phenylpentanoate (**4d**-Scheme 4): Light-yellow oil. ^{1}H NMR (300 MHz, $CDCl_3$) δ: 1.26 (t, *J* = 6.9 Hz, 3H), 1.59 (s, 3H), 2.22 (br, 1OH), 2.74 (d, *J* = 14.4 Hz, 1H), 2.85 (d, *J* = 13.2 Hz, 1H), 3.21 (ddd, *J* = 12.9, 5.4, 3.6 Hz, 1H), 3.38 (ddd, *J* = 12.9, 6.3, 3.6 Hz, 1H), 3.66 (br s, 2H), 4.00-4.17 (m, 2H), 5.26-5.30 (m, 1H), 6.05 (d, *J* = 1.8 Hz, 1H), 7.21-7.37 (m, 5H); ^{13}C NMR (75 MHz, $CDCl_3$) δ: 14.3, 22.3, 45.9, 60.9, 62.4, 63.3, 79.0, 126.5(2C), 127.3(2C), 128.3(2C), 137.5, 144.1, 168.6. HRMS (ESI-TOF) m/z: $[M+H]^+$ calcd for $C_{16}H_{23}O_4$, 279.15963; found, 279.15857.

***Tert*-butyl 3-(3-(ethoxycarbonyl)-1-(2-hydroxyethoxy)but-3-en-1-yl)-1*H*-indole-1-carboxylate** (**4e**-Scheme 4): Light-yellow oil. NMR corresponded to data reported by Chen *et al*.[26] ^{1}H NMR (300 MHz, $CDCl_3$) δ: 1.31 (t, *J* = 7.2 Hz, 3H), 1.67 (s, 9H), 2.87 (ddd, *J* = 14.1, 5.4, 1.1 Hz, 1H), 3.00 (dd, *J* = 14.0, 8.4, 1.0 Hz, 1H), 3.44 (dt, *J* = 9.9, 4.2 Hz, 1H), 3.54 (dt, *J* = 10.1, 4.0 Hz, 1H), 3.65 (br, 2H), 4.22 (q, *J* = 7.2 Hz, 2H), 4.79 (dd, *J* =8.4, 5.1 Hz, 1H), 5.57 (s, 1H), 6.18 (d, *J* = 1.5 Hz, 1H), 7.24 (td, *J* = 7.2, 1.2 Hz, 1H), 7.32 (td, *J* = 7.2, 1.5 Hz, 1H), 7.50 (s, 1H), 7.76 (d, *J* = 8.7 Hz, 1H), 8.13 (d, *J* = 8.1 Hz, 1H); ^{13}C NMR (75 MHz, $CDCl_3$) δ: 14.3, 28.3, 39.3, 61.0, 62.1, 70.1, 75.2, 84.0, 115.6, 120.2, 120.8, 122.9, 123.7, 124.7, 127.4, 128.7, 136.1, 137.6, 149.8, 167.5.

2-(2-(Benzyloxy)ethoxy)-3-hydroxyisoindolin-1-one (**7a**-Table 1): Light-yellow oil. ^{1}H NMR (500 MHz, $CDCl_3$) δ: 3.73 (ddd, *J* = 11.5, 6.5, 2.5 Hz, 1H), 3.79 (ddd, *J* = 11.5, 6.0, 2.5 Hz, 1H), 4.29 (ddd, *J* = 12.5, 7.0, 2.5 Hz, 1H), 4.42 (ddd, *J* = 12.5, 5.5, 2.5 Hz, 1H), 4.52 (d, *J* = 11.5 Hz, 1H), 4.55 (d, *J* = 11.5 Hz, 1H), 5.03 (d, *J* = 5 Hz, 1H), 5.84 (d, *J* = 5 Hz, 1H), 7.23-7.29 (m, 5H), 7.41-7.45 (m, 2H), 7.51-7.54 (m, 1H), 7.70 (d, *J* = 7.5, 1H); ^{13}C NMR (125 MHz, $CDCl_3$) δ: 68.5, 73.5, 76.5, 83.0, 123.6, 123.8, 128.2(2C), 128.4, 128.8(2C), 129.3, 130.1, 133.3, 137.1, 141.0, 166.0. HRMS (ESI-TOF) m/z: $[M+H]^+$ calcd for $C_{17}H_{18}NO_4$, 300.12358; found, 300.12465.

http://dx.doi.org/10.29356/jmcs.v70i1.2527

J. Mex. Chem. Soc. **2026**, *70(1):e2527*
Regular Issue

ISSN-e 2594-0317

Results and discussion

Cyclic voltammetry analysis of compounds 3

Previous synthetic and electroanalytical (cyclic voltammetry, CV) studies demonstrated an irreversible cathodic peak around –1.6 V vs Ag/Ag^+, corresponds to the formation of a radical anion intermediate of the *N*-alkyloxyphthalimide moiety, which undergoes homolytic *N–O* bond cleavage. This feature has been used to generate carbonyl products *via* either intramolecular elimination or cage-cluster collapse mechanisms. [21,22]

However, despite the proven ability of NAPIs as alkoxyl radical precursors, their electrochemical behavior had not been thoroughly explored until the present study. The cyclic voltammetry of the synthesized NAPIs (**3a-3e**) was carried out, revealing that all substrates exhibited an irreversible reduction peak, consistent with the previously reported value for NBOPIs (Fig. 1). This finding suggests a similar initial electron transfer process, leading to the formation of the corresponding radical anion. The second cathodic peak (–2.8 V vs Ag/Ag^+), is attributed to the reduction of the phthalimide moiety, a feature also reported in prior mechanistic studies.[21,22] Thus, the occurrence of these peaks supports an initial reduction of the *N*-alkoxyphthalimide to form a reactive radical anion, which undergoes homolytic *N-O* bond cleavage to generate the corresponding alkoxyl radical and a phthalimide reduced moiety. Consistently, the NAPIs tested (**3a-3b**, **3d-3e**) exhibited a two-step reductive behavior in their cyclic voltammograms. The subtle differences observed among the cathodic voltammograms are attributed to substituent-dependent electronic effects that modulate the stability of the reduced intermediates and the efficiency of the subsequent *N-O* bond fragmentation, as has been reported for NBOPIs systems. [21,22] In contrast, the fluorinated derivative **3c** lacks the characteristic second cathodic peak. Considering the relatively accessible reduction potential associated with aryl-CF_3 moieties, an alternative or competing reduction process involving the trifluoromethyl-substituted aromatic system may occur, thereby inhibiting the desired *N-O* bond fragmentation pathway.[29,31] This behavior is consistent with the low reactivity observed for **3c** under the electrosynthetic conditions (*vide infra*) and further highlights the influence of substituents on the reduction pathway of NAPIs. The oxidation peak observed in some compounds is tentatively attributed to the benzylic position oxidation, but further experiments are required to confirm this.

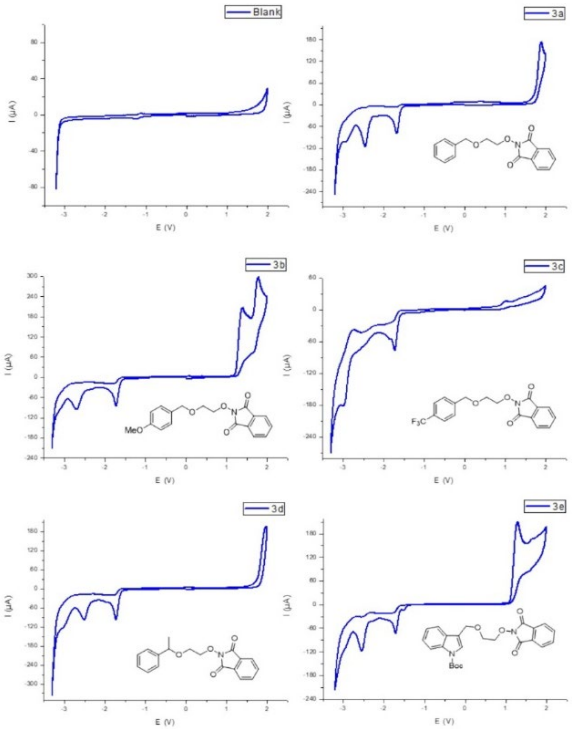

Fig. 1. Cyclic voltammetry of selected *N*-alkoxyphthalimides **3a-3e** (4 mM). 0.1 M n-Bu_4NPF_6 in CH_3CN, at 0.1 Vs^{-1}. WE: Glassy carbon, CE: Pt, RE: Ag/Ag^+.

http://dx.doi.org/10.29356/jmcs.v70i1.2527

J. Mex. Chem. Soc. **2026**, *70(1):e2527*
Regular Issue

ISSN-e 2594-0317

Electrotransformation of compounds 3

N-alkoxyphthalimide **3a** was selected as a model substrate to access the allylated product **4a** under RAP electrolysis conditions, using Hantzsch ester as hydrogen donor and ethyl 2-((phenylsulfonyl)methyl)acrylate as the radical acceptor, in CH_2Cl_2. First, to promote the intermolecular interaction between the entities involved, the reaction concentration was increased to 0.05 M and 0.1 M, showing a yield of 19 % and no reaction in the latter because of poor solubility of the reagents (Table 1, entries 1-2). Diverse solvents and solvent mixtures were used; the mixture of renewable THF and acetonitrile (9:1) gave a good yield, as DCM (entries 3-6). The low and high rates of polarity switching did not improve the yield of **4a** (entries 7-8). Surprisingly, using a different mode to alternate the polarity, pulsed alternating polarity (PAP)[32,33] electrolysis (entry 9). Compared to previous experiments, the formation of a thin film on the electrode surface was not observed, which may contribute to the diminished effectiveness of the redox processes. Carrying out the reaction under low current density did not lead to the consumption and conversion of **3a**; meanwhile, the reduction of employed charge gave a low yield of the desired product (entries 10-11). Considering the relevance of charging and discharging electrode processes, the platinum electrode showed a favorable result compared to the G.C. electrode when DCM was used as a solvent (entries 12-13).[34] On the other hand, the substitution of HE (entry 14), or combination with other electron/H-atom donors (entries 15-19)[35] showed a better result, thus when γ-terpinene was added (entries 17-19) and with 1 eq. HE an improved formation of **4a** was observed (entry 18). Under the electrochemical conditions employed, the roles of Hantzsch ester and γ-terpinene are expected to be complementary. Hantzsch ester likely functions as a sacrificial reductant, participating in electron-transfer events and facilitating subsequent delivery to anion radical intermediates. In contrast, γ-terpinene is proposed to act primarily as a hydrogen-atom donor and radical quencher, mitigating unproductive radical pathways and stabilizing reactive species generated during electrolysis.[36,37] The cooperative action of these additives is therefore critical for controlling radical reactivity and promoting productive allylation.

Table 1. Screening conditions for electrochemical C-H functionalization of **3a**.

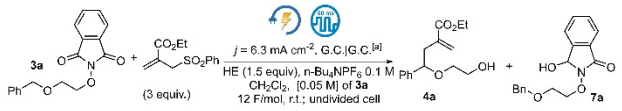

Entry	Variations	Yield of 4a[b]
1	None	19 %
2	[0.1 M] of **3a**	N.R.[c][d]
3	CH_3CN	N.R.
4	Dioxane	N.R.
5	2-Me-THF	17 %
6	2-Me-THF/CH_3CN	22 %
7	2-Me-THF/CH_3CN; 25 ms	0 %[e]
8	2-Me-THF/CH_3CN; 100 ms	0 %[d]
9	2-Me-THF/CH_3CN; PAP	19 %
10	2-Me-THF/CH_3CN; PAP; j = 3 mA cm^{-2}	N.R.
11	2-Me-THF/CH_3CN; PAP; 8 F/mol	13 %

http://dx.doi.org/10.29356/jmcs.v70i1.2527

J. Mex. Chem. Soc. **2026**, *70(1):e2527*
Regular Issue

ISSN-e 2594-0317

12	2-Me-THF/CH_3CN; PAP; Pt electrodes	0 %[e]
13	PAP; Pt electrodes	24 %
14	PAP; Pt electrodes; Ac. Formic (10 eq)/Bu_3N (10 eq)	0 %[e]
15	PAP; Pt electrodes; HE (2 eq)/Bu_3N (2 eq)	0 %[e]
16	PAP; Pt electrodes; HE (1.5 eq)/1,4-cyclohexadiene (10 eq)	0 %[e]
17	PAP; Pt electrodes; HE (1.5 eq)/γ-terpinene (10 eq)	30 %
18	PAP; Pt electrodes; HE (1 eq)/γ-terpinene (10 eq)	38 %
19	PAP; Pt electrodes; HE (0 eq)/γ-terpinene (10 eq)	0 %[e]

[a] G.C.=Glassy carbon. [b] Determined by NMR. [c] N.R. = No reaction, starting material recovered. [d] The overreduction-hydroxylactam product **7a**[38] was detected. [e] A complex mixture of byproducts was observed by TLC.

Although alternative solvents were evaluated, CH_2Cl_2 provided the best compromise between substrate solubility, electrochemical stability, and reaction reproducibility. Other solvents led to lower conversions or more complex reaction mixtures, preventing their practical application under the studied conditions. The optimized reaction conditions, the NAPIs **3b**-**3e** were tested under conditions of entry 18. The presence of an electron-donating group on the aryl moiety provided the highest yield of the allylated product **4b**, without formation of cyclic dioxane-type byproducts, likely due to the reduced oxidation of the benzylic radical. In contrast, the substrate bearing a CF_3 group did not afford the desired product. The steric barrier of a methyl group in the benzylic position did not inhibit hydrogen abstraction but rather diminished the product yield (Scheme 4**(a)**, Eq. 1); meanwhile, the indole framework showed compatibility under the electrochemical conditions (Scheme 4**(a)**, Eq. 2). Finally, to compare the formation of allylated products **4a**-**4e** with photocatalytic redox conditions,[39] the corresponding NAPIs **3a**-**3e** were reacted under parameters described in scheme 4**(b)**, showing similar yields of compounds **4** than those found in the electrochemical reaction.

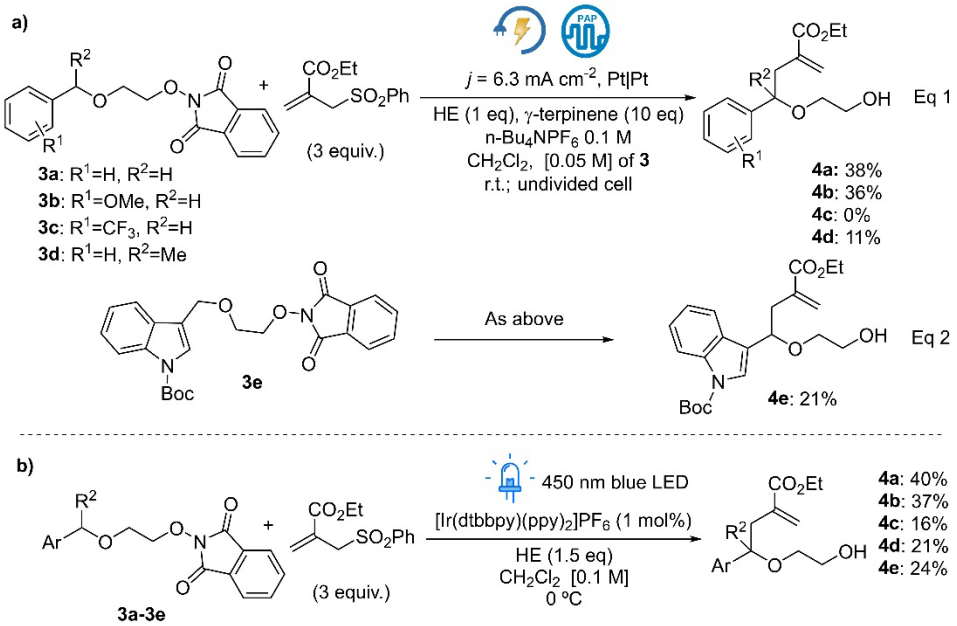

Scheme 4. *C-H* allylation of NAPIs under **(a)** electrochemical, and **(b)** photocatalytic redox conditions.

J. Mex. Chem. Soc. **2026**, *70(1):e2527*
Regular Issue

ISSN-e 2594-0317

When comparing the two activation modes, photoredox functionalization of **3a-3e** afforded slightly higher conversions in shorter reaction times (Table 2) but required continuous external light irradiation and active temperature control using a recirculating chiller. By contrast, the electrosynthetic protocol operates under low-current and moderate-voltage conditions, resulting in a relatively low overall electrical energy input despite longer electrolysis times.

Table 2. Charge and/or time employed in the C-H allylation of **3a-3e**.[a]

Entry	Substrate	Modality	Equipment energy demand	Time (h mmol^{-1})	Charge (C mmol^{-1})
1	**3a-3e**	Electro (PAP)	ElectraSyn (39.84 W)	45.9	1158
2	**3a-3e**	Photo (Ir (III))	Blue LED (18W) Stirring plate (30W) Recirculating chiller (250W)	10	-

[a] All values were normalised to time per mmol and charge per mmol. See SI for experimental and calculation details.

Conclusions

The use of the rapid alternating polarity electrolysis technique to generate alkoxyl radicals from *N*-alkoxyphthalimides proved compatible with enabling 1,5-hydrogen atom transfer and the subsequent intermolecular capture of the transient benzylic radical. As previously reported, cyclic voltammetry studies of NAPIs revealed similar reduction peaks to those observed with NBOPIs; however, the presence of a deactivating group led to degradation of the starting material. Furthermore, the products obtained have been demonstrated to be competitive with the accepted PRC approach. These findings exhibit that electrochemical approaches can effectively bypass the need for expensive and scarce transition metals, offering a viable and sustainable alternative.[40] Both methodologies avoid toxic stannyl reagents, supporting electrochemistry as a more sustainable alternative; however, the use of CH_2Cl_2, tetraalkylammonium salts, and high charge consumption highlights opportunities for further improvement. Given their compatibility with radical-based reactivity, such protocols represent a valuable tool for modern synthetic chemistry, particularly in the pharmaceutical industry.

Acknowledgements

B.A.F.-U. express their gratitude to CONAHCyT for the financial support of the project (Grant A1-S-18230). E.A.C.-D. acknowledges CONAHCyT for the scholarship. D.F.C.-B. acknowledges CONAHCyT for the doctoral scholarship (2020-000026-02NACF-22248). J.R.I. acknowledges DGAPA-UNAM for the postdoctoral fellowship (UNAM Posdoctoral Program - POSDOC). We thank M. Sc. María de las Nieves Zavala-Segovia, M. Sc. Carmen García, M.Sc. Lizbeth Triana and M.C.S. María Citlalit Martínez Soto for the technical support provided.

References

1. Ali, M.; Sewell, S.; Li, J.; Wang, T. *Organics.* **2023**, *4*, 459–489. DOI: https://doi.org/10.3390/org4040033
2. Jia, K.; Chen, Y. *Chem. Commun*. **2018**, *54*, 6105-6112. DOI: https://doi.org/10.1039/C8CC02642D

J. Mex. Chem. Soc. **2026**, *70(1):e2527*
Regular Issue

ISSN-e 2594-0317

3. Litwinienko, G.; Beckwith, A.L.J.; Ingold, K.U. *Chem. Soc. Rev.* **2011**, *40*, 2157–2163. DOI: https://doi.org/10.1039/C1CS15007C
4. Salamone, M.; Bietti, M. *Synlett*. **2014**, *25*, 1803–1816. DOI: https://doi.org/10.1055/s-0033-1341280
5. Hartung, J.; Gottwald, T.; Špehar, K. *Synthesis*. **2002**, 1469-1498. DOI: https://doi.org/10.1055/s-0033-1341280
6. Banoun, C.; Magnier, E.; Dagousset, G. *Synlett*. **2024**, *35*, 268-278. DOI: https://doi.org/10.1055/a-2131-4126
7. Morcillo, S.P. *Angew. Chem. Int. Ed*. **2019**, *58*, 14044-14054. DOI: https://doi.org/10.1002/anie.201905218
8. Bietti, M.; Lanzalunga, O.; Salamone, M. *J. Org. Chem*. **2005**, *70*, 1417-1422. DOI: https://doi.org/10.1021/jo048026m
9. Salomone, M.; Bietti, M. *Acc. Chem. Res*. **2015**, *48*, 2895−2903. DOI: https://doi.org/10.1021/acs.accounts.5b00348
10. Stateman, L.M.; Nakafuku, K.M.; Nagib, D.A. *Synthesis*. **2018**, *50*, 1569–1586. DOI: https://doi.org/10.1055/s-0036-1591930
11. Luo, Y.-R., in: *Comprehensive Handbook of Chemical Bond Energies*; CRC Press: Boca Raton, FL, **2007**. DOI: https://doi.org/10.1201/9781420007282
12. Chang, L.; An, Q.; Duan, L.; Feng, K.; Zuo, Z. *Chem. Rev*. **2022**, *122*, 2429−2486. DOI: https://doi.org/10.1021/acs.chemrev.1c00256
13. El Gehani, A.A.M.A.; Maashi, H.A.; Harnedy, J.; Morril, L.C. *Chem. Commun.* **2023**, *59*, 3655-3664. DOI: https://doi.org/10.1039/D3CC00302G
14. Budnikov, A.S.; Krylov, I.B.; Lastovko, A.V.; Yu, B.; Terent'ev, A.O. *Asian J. Org. Chem*. **2022**, *11*, e202200262. DOI: https://doi.org/10.1002/ajoc.202200262
15. Liu, J.; Jin, J.; Zhang, K.; Cai, L. *Asian J. Org. Chem.* **2023**, *12*, e202300160. DOI: https://doi.org/10.1002/ajoc.202300160
16. Kim, S.; Lee, T.A.; Song, Y. *Synlett*. **1998**, 471-472. DOI: https://doi.org/10.1055/s-1998-1711
17. Crespi, S.; Fagnoni, M. *Chem. Rev*. **2020**, *120*, 9790−9833. DOI: https://doi.org/10.1021/acs.chemrev.0c00278
18. Chatgilialoglu, C.; Ferreri, C.; Landais, Y.; Timokhin, V.I. *Chem. Rev*. **2018**, *118*, 6516−6572. DOI: https://doi.org/10.1021/acs.chemrev.8b00109
19. Frontana-Uribe, B.A.; Little, R.D.; Ibanez, J.G.; Palma, A.; Vasquez-Medrano, R. *Green Chem*. **2010**, *12*, 2099–2119. DOI: https://doi.org/10.1039/C0GC00382D
20. Cembellín, S.; Batanero, B. *Chem. Rec.* **2021**, *21*, 2453–2471. DOI: https://doi.org/10.1002/tcr.202100128
21. Syroeshkin, M.A.; Krylov, I.B.; Hughes, A.M.; Alabugin, I.V.; Nasybullina, D.V.; Sharipov, M.Y.; Gultyai, V.P.; Terent'ev, A.O. *J. Phys. Org. Chem*. **2017**, *30*, e3744. DOI: https://doi.org/10.1002/poc.3744
22. Chicas-Baños, D.F.; López-Rivas, M.; Gonzalez, F.J.; Sartillo-Piscil, F.; Frontana-Uribe, B.A. *Heliyon*. **2024**, *10*, e23808. DOI: https://doi.org/10.1016/j.heliyon.2023.e23808
23. Romero-Ibañez, J.; Chicas-Baños, D.F.; Sartillo-Piscil, F.; Frontana-Uribe, B.A. *Curr. Res. Green Sustain. Chem*. **2024**, *8*, 100404. DOI: https://doi.org/10.1016/j.crgsc.2024.100404
24. Fu, X.; Ran, T.; Liu, J. *Org. Chem. Front*. **2024**, *11*, 6760-6767. DOI: https://doi.org/10.1039/D4QO01607F
25. Ibanez, J.G.; Frontana-Uribe, B.A.; Vasquez-Medrano, R. *J. Mex. Chem. Soc*. **2016**, *60*, 247-260. DOI: https://doi.org/10.29356/jmcs.v60i4.117
26. Zhang, J.; Li, Y.; Zhang, F.; Hu, C.; Chen, Y. *Angew.Chem. Int. Ed*. **2016**, *55*, 1872–1875. DOI: https://doi.org/10.1002/anie.201510014
27. Minke, C.; Suermann, M.; Bensmann, B.; Hanke-Rauschenbach, R. *Int. J. Hydrog. Energy*. **2021**, *46*, 23581-23590. DOI: https://doi.org/10.1016/j.ijhydene.2021.04.174

J. Mex. Chem. Soc. **2026**, *70(1):e2527*
Regular Issue

ISSN-e 2594-0317

28. White, A.R.; Kozlowski, R.A.; Tsai, S.-C.; Vanderwal, C.D. *Angew.Chem. Int. Ed*. **2017**, *56*, 10525-10529. DOI: https://doi.org/10.1002/anie.201704119
29. Andrieux, C.P.; Combellas, C.; Kanoufi, F.; Savéant, J.-M.; Thiébault, A. *J. Am. Chem. Soc*. **1997**, *119*, 9527-9540. DOI: https://doi.org/10.1021/ja971094o
30. Box, J.R.; Avanthay, M.E.; Poole, D.L.; Lennox, A.J.J. *Angew. Chem. Int. Ed*. **2023**, *62*, e202218195. DOI: https://doi.org/10.1002/anie.202218195.
31. Mena, S.; Bernad, J.; Guirado, G. *Catalysts*. **2021**, *11*, 880. DOI: https://doi.org/10.3390/catal11080880
32. IKA. ElectraSyn 2.0 Electrochemistry Kit; https://www.ika.com/en/Products-LabEq/Electrochemistry-Kit-pg516/; accessed in August 2025.
33. Atkins, A.P.; Lennox, A.J.J. *Curr. Opin. Electrochem*. **2024**, *44*, 101441. DOI: https://doi.org/10.1016/j.coelec.2024.101441
34. Jamshidi, M.; Fastie, C.; Hilt, G. *Synthesis*. **2022**, *54*, 4661-4672. DOI: https://doi.org/10.1055/s-0042-1751367
35. Nguyen, J.D.; D'Amato, E.M.; Narayanam, J.M.R.; Stephenson, C.R.J. *Nature Chem*. **2012**, *4*, 854-859. DOI: https://doi.org/10.1038/nchem.1452
36. de Pedro Beato, E.; Spinnato, D.; Zhou, W.; Melchiorre, P. *J. Am. Chem. Soc*. **2021**, *143*, 12304-12314. DOI: https://doi.org/10.1021/jacs.1c05607
37. Leone, M.; Arnaldi, D.; Fagnoni, M. *Org. Chem. Front*. **2025**, *12*, 4970-4979. DOI: https://doi.org/10.1039/D5QO00399G
38. Bai, Y.; Shi, L.; Zheng, L.; Ning, S.; Che, X.; Zhang, Z.; Xiang, J. *Org. Lett*. **2021**, *23*, 2298−2302. DOI: https://doi.org/10.1021/acs.orglett.1c00430
39. Xochicale-Santana, L.; Cortezano-Arellano, O.; Frontana-Uribe, B.A.; Jimenez-Pérez, V.M.; Sartillo Piscil, F. *J. Org. Chem.* **2023**, *88*, 4880-4885. DOI: https://doi.org/10.1021/acs.joc.3c00251
40. Romero-Ibañez, J.; Guarneros-Cruz, K.A.; Sartillo-Piscil, F.; Frontana-Uribe, B.A. *ChemSusChem*. **2025**, *18*, e202501605. DOI: https://doi.org/10.1002/cssc.202501605